

IC/94/203  
TAUP-2183-94  
August 1994

# Radiative Corrections for Pion Polarizability Experiments

A. A. Akhundov<sup>1,2</sup>, S. Gerzon<sup>3</sup>, S. Kananov<sup>3</sup>, M. A. Moinester<sup>3</sup>

<sup>1</sup> *International Centre for Theoretical Physics, 34014 Trieste, Italy*

<sup>2</sup> *Institute of Physics, Azerbaijan Academy of Sciences, 370143 Baku, Azerbaijan*

<sup>3</sup> *Raymond and Beverly Sackler Faculty of Exact Sciences,  
School of Physics and Astronomy, Tel Aviv University,  
69978 Ramat Aviv, Israel*

## Abstract

We use the semi-analytical program RCFORGV to evaluate radiative corrections to one-photon radiative emission in the high-energy scattering of pions in the Coulomb field of a nucleus with atomic number Z. It is shown that radiative corrections can simulate a pion polarizability effect. The average effect is  $\alpha_{\pi}^{rc} = -\beta_{\pi}^{rc} = (0.20 \pm 0.05) \times 10^{-43} \text{ cm}^3$ , for pion energies 40-600 GeV. We also study the range of applicability of the equivalent photon approximation in describing one-photon radiative emission.

# 1 Introduction

Pion electric  $\bar{\alpha}$  and magnetic  $\bar{\beta}$  Compton polarizabilities [1]-[4] characterize the induced transient dipole moments of pion subjected to external oscillating electric  $\vec{E}$  and magnetic  $\vec{H}$  fields. The polarizabilities can be obtained from precise measurements of the gamma-pion Compton scattering differential cross section. They probe the rigidity of the internal structure of the pion, since they are induced by the rearrangement of the pion constituents via action of the photon electromagnetic fields during scattering. For the  $\gamma\pi$  interaction at low energy, chiral symmetry provides a rigorous way to make predictions. This approach [5, 6] yields  $\bar{\alpha}_\pi = -\bar{\beta}_\pi = 2.7 \pm 0.4$  (in units  $10^{-43} \text{ cm}^3$ ).

The radiative scattering of high energy pions in the Coulomb field of a nucleus [7]:

$$\pi(p_1) + Z(p) \rightarrow \pi(p_2) + Z(p') + \gamma(k'), \quad (1)$$

determines the  $\gamma\pi$  Compton scattering:

$$\pi(p_1) + \gamma(k) \rightarrow \pi(p_2) + \gamma(k'). \quad (2)$$

The  $\gamma\pi$  scattering was measured [8, 9] with 40 GeV pions at Serpukhov via the Primakoff radiative scattering process (1). The incident pion scatters from a virtual photon, characterized by 4-momentum  $k = p - p'$ ; and the final state gamma ray and pion are detected in coincidence. The pion electric polarizability  $\bar{\alpha}_\pi$  was deduced in a low statistics ( $\sim 7$  000 events) experiment to be:

$$\bar{\alpha}_\pi = -\bar{\beta}_\pi = 6.8 \pm 1.4_{\text{stat}} \pm 1.2_{\text{syst}}. \quad (3)$$

It was assumed in the analysis that  $\bar{\alpha}_\pi + \bar{\beta}_\pi = 0$ , as expected theoretically [5]. This result differs from the chiral prediction by more than two standard deviations. The experimental situation points to the need for much higher quality data and more attention to the systematic uncertainties arising from different measurement and analysis techniques. A new Primakoff experiment is planned at FNAL [10].

In the lowest order, the process of the radiative scattering of the pions in the Coulomb field of a nucleus is described by Feynman graphs of Fig. 1: <sup>1</sup> 1a) the QED interaction of the pointlike pion with the electromagnetic field of the nucleus; 1d) the two-photon interaction of the pion, including the structure effects described by the polarizabilities of the pion. In the next order of  $\alpha$ , there are contributions from the QED processes presented in Fig. 1(b,c). The double bremsstrahlung process (1c):

$$\pi(p_1) + Z(p) \rightarrow \pi(p_2) + Z(p') + \gamma(k_1) + \gamma(k_2), \quad (4)$$

and the one-loop diagrams (1b) with the virtual photon, both contribute to the measured cross section of the reaction (1).

The total cross section for the radiative scattering process (1) can be written in the form:

$$d\sigma^{\text{tot}} = d\sigma^{\text{Born}} + d\sigma^{\text{pol}} + d\sigma^{\text{rc}}. \quad (5)$$

Here,  $d\sigma^{\text{Born}}$  corresponds to scattering of a pointlike pion in the Born approximation, and the following terms give the contributions of the structure effects (linear terms in the pion polarizability) and the radiative corrections. The radiative corrections are important for high statistics experiments, and are needed to extract the Compton cross sections from data. The

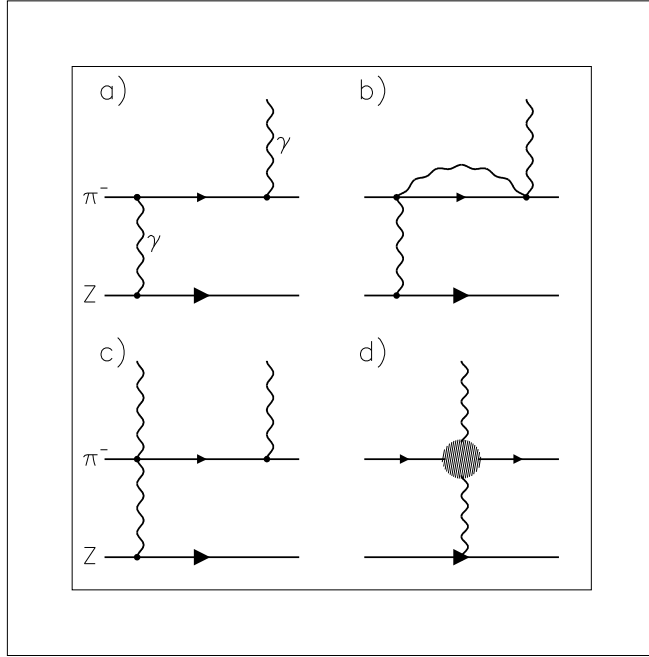


Figure 1: *Feynman graphs for radiative scattering of pions on Coulomb center: a) the Born approximation; b) the one-loop QED corrections; c) the double photon bremsstrahlung; d) the structure effects - pion polarizabilities.*

experimental data can be interpreted in terms of polarizabilities, only after accounting for the radiative corrections.

The theoretical investigation [11]-[13] of these radiative corrections (RC) was undertaken initially for the analysis of the experiment [8, 9] of JINR (Dubna) and IHEP (Serpukhov). It was shown that the detailed properties of the gamma detector are important; such as the photon detector threshold, energy and position resolution, and the two-photon angular resolution. For the setup of Antipov *et al.* [8, 9] at 40 GeV, the radiative corrections were estimated to affect polarizability determinations at the level of  $\sim 3\%$  [13].

In this note we present a study of the radiative corrections to the process (1) at higher energies and for higher  $Z$  targets. Our calculations were carried out with the semi-analytical program RCFORGV [14].

## 2 The semi-analytical program RCFORGV

The analytical formulae for the RC to the inclusive spectra of the scattering of a spinless point-like particle by a Coulomb center with emission of a hard photon were obtained in [11, 13]. The contribution of the QED one-loop corrections (Fig. 1b) and of the double bremsstrahlung from pions (Fig. 1c) were calculated exactly without any approximation and for  $m_\pi \neq 0$ . The calculation of the Feynman diagrams was carried out using the program SCHOONSCHIP [15], which allows the relevant algebraic manipulations and analytic transformations. The other

<sup>1</sup>In Fig. 1, only one of the full set of needed diagrams is presented.

important contribution from higher order processes corresponds to the QED rescattering processes in which the scattering pion interacts with the electromagnetic field by exchange of two virtual photons. The calculations of the rescattering cross section lead to the analytic results presented in [12].

These formulae were incorporated into the Fortran code RCFORGV [14]. The RCFORGV program calculates more than 100 contributions from the 43 Feynman graphs, that are needed to describe the pion scattering by nuclei: 3 diagrams in the Born approximation, one graph for the structure effects (polarizability), and 39 diagrams for the radiative corrections. The numerical calculations in the RCFORGV program are performed by the Monte Carlo method. Double precision numbers are necessary for the calculations of the contribution of the double bremsstrahlung process (4). The program package RCFORGV is set up on a IBM-3072 at Tel Aviv University.

The semi-analytical program RCFORGV calculates the radiative corrections of order  $\mathcal{O}(\alpha)$  to the process (1) for the following cross sections:

- i) for  $d\sigma/d\omega$  in the  $\omega$ -bins :  $\omega = E_1 - E_2$ ;
- ii) for  $d^2\sigma/dE_2dQ^2$  in the points of  $(E_2, Q^2)$  .

Here  $Q^2 = -(p_1 - p_2)^2$ , and  $E_1$  ( $E_2$ ) are the initial (final) energies of the pions in the laboratory system. These cross sections are needed to the analysis of planned experiments.

In RCFORGV, it is easy to provide a variety of kinematic cuts and criteria for event selection, and to take into account the experimental geometry. The following kinematic constraints are included in the program:

- 1)  $t = -k^2 = -(p_1 - p_2 - k')^2 < \bar{t}$  for the 4-momentum transfer ;
- 2)  $\theta_\pi < \bar{\theta}_\pi$  for the pion scattering angle in the laboratory frame;
- 3)  $\omega > \bar{\omega}$  for the photon detection threshold;
- 4)  $\theta_{\gamma\gamma} > \bar{\theta}_{\gamma\gamma}$  for the angular resolution of the double bremsstrahlung.

Here  $\bar{t}$  is the maximum value of the squared momentum transfer, fixed by experimental resolution in  $t$ . Below  $\bar{t}$ , Coulomb scattering dominates [7]. Also,  $\bar{\theta}_\pi$  is the maximum of the pion scattering angle. The parameters  $\bar{\omega}$  and  $\bar{\theta}_{\gamma\gamma}$  are important for distinguishing double and single bremsstrahlung. If  $\omega < \bar{\omega}$  or  $\theta_{\gamma\gamma} < \bar{\theta}_{\gamma\gamma}$ , then these two processes are indistinguishable [12].

Using RCFORGV, the cross sections at the energies 40 and 600 GeV for the radiative scattering of  $\pi^-$  mesons on carbon, were calculated in the Born approximation (the Born cross section), including polarizability contributions and radiative corrections. Numerical calculations were performed by the Monte Carlo method, using 50 000 events for each incident energy. The value 40 GeV was chosen to test our new program installation with results given previously in [13]. One set of calculations was done for lead, to investigate the Z dependence. The cross sections were calculated with kinematic constraints given in Table 1.

These constraints take into account the geometry and the event selection criteria for experiments [8] and [10]. Due to kinematics, we chose the parameters of  $\bar{t}$  and  $\bar{\omega}$  larger, and angles  $\bar{\theta}_\pi$  and  $\bar{\theta}_{\gamma\gamma}$  smaller, for energy 600 GeV compared to 40 GeV.

Energy	Parameters			
	$\bar{t}$	$\bar{\omega}$	$\theta_\pi$	$\theta_{\gamma\gamma}$
GeV	GeV <sup>2</sup>	GeV	rad	rad
40	$2 \times 10^{-4}$	0.5	$1.5 \times 10^{-2}$	$2.0 \times 10^{-3}$
600	$4 \times 10^{-3}$	10.0	$7.0 \times 10^{-3}$	$2.0 \times 10^{-4}$

Table 1: *The kinematic constraints used in the program RCFORGV.*

### 3 The role of radiative correction

In this section we present the RCFORGV calculations. Following [12], we define the radiative correction factor  $\delta(\omega)$  as the ratio of the radiative corrections cross section to the Born cross section, as a function of the detected gamma energy  $\omega$ :

$$\delta(\omega) = \frac{(d\sigma/d\omega)^{rc}}{(d\sigma/d\omega)^{Born}}. \quad (6)$$

The results of the RC calculations for the radiative scattering of 40 GeV and 600 GeV  $\pi^-$  mesons on carbon nuclei are presented in Fig. 2. One sees that the absolute value of  $\delta(\omega)$  is

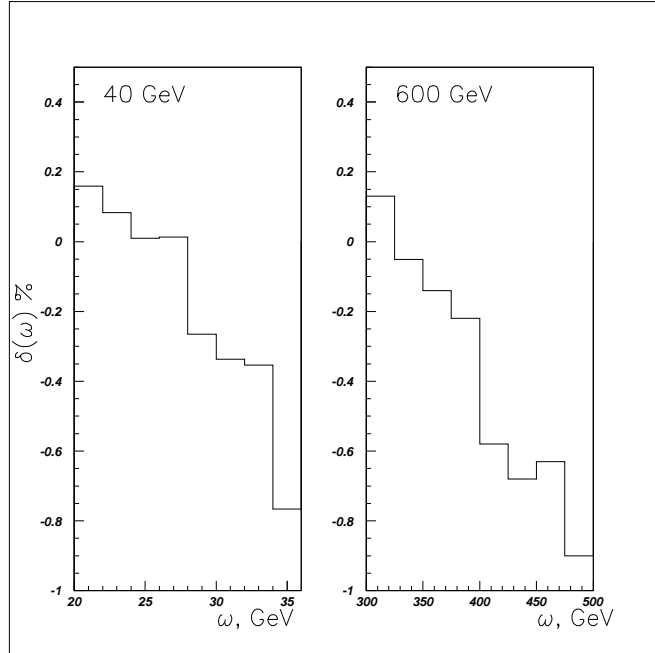


Figure 2: *Radiative correction  $\delta(\omega)$  for radiative scattering of 40 and 600 GeV  $\pi^-$ -mesons on  $C^{12}$  nuclei.*

less than 1% over a large energy range.

The polarizability cross section can be written as the sum of two terms [13]:

$$d\sigma^{pol} = -(\bar{\alpha}_\pi + \bar{\beta}_\pi)d\sigma^e + \bar{\beta}_\pi d\sigma^m, \quad (7)$$

where  $d\sigma^e$  and  $d\sigma^m$  give different combinations of electric and magnetic polarizabilities. We imposed the condition  $\bar{\alpha}_\pi + \bar{\beta}_\pi = 0$ . In our analysis, we therefore determine radiative corrections with respect to one polarizability value  $\bar{\alpha}_\pi = -\bar{\beta}_\pi$ . To set the scale, we used the values:

$$\bar{\alpha}_\pi = -\bar{\beta}_\pi = 5. \quad (8)$$

The ratio of the radiative correction cross section to polarizability cross section is presented in Fig. 3. This ratio changes in the interval  $\sim (-5; 5)\%$  as function of gamma energy  $\omega$ . The

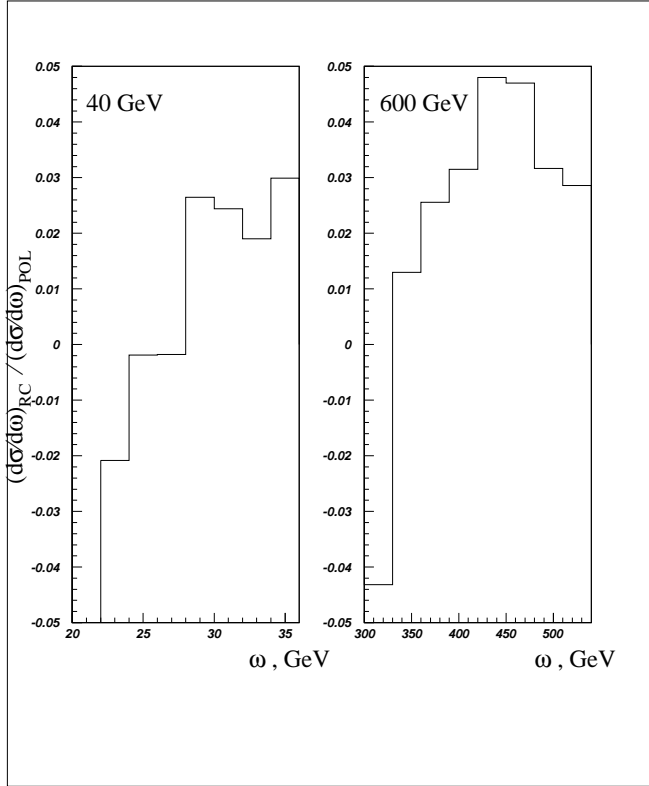


Figure 3: *Ratio of the radiative correction to the polarizability cross section for radiative scattering of 40 and 600 GeV  $\pi^-$ -mesons on  $C^{12}$  nuclei.*

formula (5) can be written:

$$d\sigma^{tot} = d\sigma^{Born} + \bar{\beta}_\pi d\sigma^m + d\sigma^{rc}. \quad (9)$$

To emphasize the fact that radiative corrections can simulate a polarizability, we rewrite (9):

$$d\sigma^{tot} = d\sigma^{Born} + (\bar{\beta}_\pi + \beta_\pi^{rc}) d\sigma^m, \quad (10)$$

where  $\beta_\pi^{rc} = d\sigma^{rc}/d\sigma^m$ .

In this analysis, we calculate also the double differential cross section  $d^2\sigma/dE_2 dQ^2$ . We can transform this cross section to the center mass of the  $\gamma\pi$  system, as  $d^2\sigma/ds_1 d\cos\theta^*$ . Here,  $s_1 = (p_1 + k)^2 = (p_2 + k')^2$  and  $\theta^*$  are the  $\gamma\pi$  energy squared, and the Compton scattering angle. At very small  $-k^2 \leq \bar{t}$  and small  $\theta_\pi \leq \bar{\theta}_\pi$  we find:

$$\frac{d^2\sigma}{ds_1 d\cos\theta^*} = \frac{E_1(s_1 - m_\pi^2)^2 (1 - \cos\theta^*)}{4s_1^2} \frac{d^2\sigma}{dE_2 dQ^2}. \quad (11)$$

The ratio of the polarizability to the Born double differential cross section for different scattering angles, as a function of  $s_1$ , is presented in Fig. 4a. In this figure ratios of  $d^2\sigma/dE_2dQ^2$  were taken, but the labeling is according to the CM variables  $s_1$  and  $\cos\theta^*$ . It is seen that the absolute value of the polarizability contribution increases with energy and can reach a value of  $\sim 30\%$  at backward angles. For a gamma energy  $\omega^* = (s_1 - m_\pi^2)/2\sqrt{s_1} \approx 150\text{MeV}$  and  $\cos\theta^* \approx -0.5$ , the contribution of magnetic polarizability to the total cross section of reaction (1) is about 7%. At the point  $s_1 = 0.18\text{GeV}^2$  ( $\omega^* \approx 200\text{MeV}$ ) and  $\cos\theta^* = -0.95$ , this contribution attains magnitude of  $\sim 30\%$ . In the laboratory frame, this kinematical range corresponds to the range of detected gamma energies  $\omega \sim (0.60 - 0.90)E_1$ , where

$$\omega = \frac{E_1}{2}(1 - \frac{m_\pi^2}{s_1})(1 - \cos\theta^*). \quad (12)$$

Here, we point out that data of [8, 9] were taken in this region of  $\omega$  as well. These authors showed that the preferred kinematical range to study the magnetic polarizability in the laboratory frame is the range of final gamma energy  $\omega \geq 0.75E_1$ . In the center of mass frame, this region is defined by the inequalities:  $s_1 \geq 0.15\text{GeV}^2$  and  $\cos\theta^* \leq -0.75$ . One sees from Fig. 4a that for this kinematical range, the relative contribution of magnetic polarizability to the Born cross section is more than 15%. In Fig. 4b, the ratio of the RC to polarizability double differential cross section is shown. We see that the relative contribution from radiative corrections to the polarizability cross section contribution is less than 5% at backward angles for large enough values of  $s_1 \geq 0.13\text{GeV}^2$ .

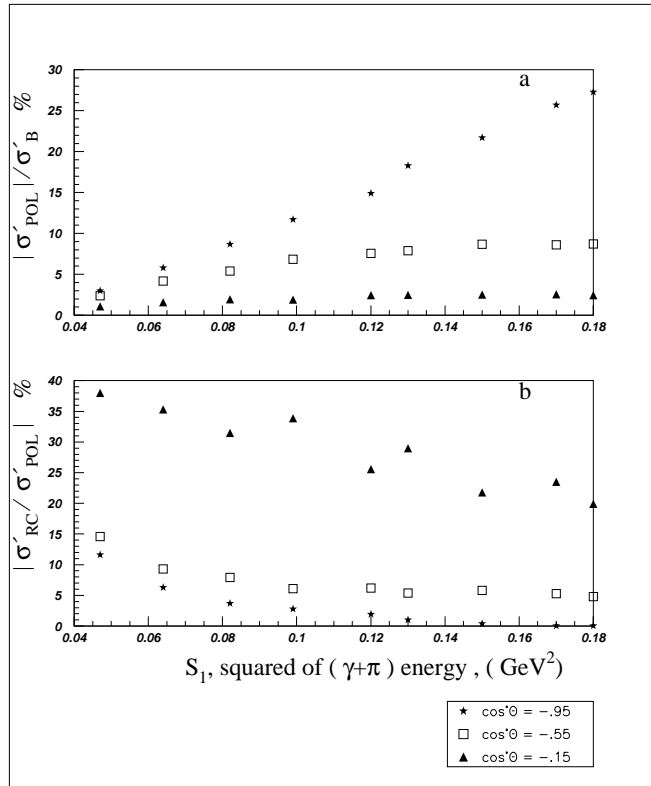


Figure 4: Ratio of  $\sigma' \equiv d^2\sigma/dE_2dQ^2$  for: a) the polarizability and the Born cross sections; b) the radiative correction and the polarizability cross sections.

We wish to determine the magnitude of the simulated contribution to the polarizability, due to the radiative corrections. We can do this by calculating the average value of the cross

section ratio  $d\sigma^{rc}/d\sigma^m$  for the gamma energy range  $\omega \geq 0.75E_1$ . We have:

$$\beta_\pi^{rc} = \frac{1}{n} \sum_{i=1}^n d\sigma^{rc}(\omega_i)/d\sigma^m(\omega_i), \quad (13)$$

where  $n$  is the number of  $\omega$  bins.

For the energies 40 and 600 GeV, we obtained  $\beta_\pi^{rc} \approx -0.20$ . The accuracy of our calculation may be estimated as:

$$\delta(\beta_\pi^{rc}) \approx \sqrt{n} \epsilon_{tot} \beta_\pi^{rc}, \quad (14)$$

where  $\epsilon_{tot} = \sqrt{\epsilon_{rc}^2 + \epsilon_{pol}^2}$ . Here,  $\epsilon_{rc}$  and  $\epsilon_{pol}$  are the relative uncertainties in the radiative correction and polarizability cross section calculations. These uncertainties were calculated by the RCFORGV program for each of  $\omega$  bins and we have found that over the gamma energy range  $\omega \geq 0.75E_1$  all of  $\epsilon_{tot}$  are approximately the same. This fact explains the appearance of  $\sqrt{n}$  in (14). We have obtained  $\epsilon_{tot} \approx 0.12$ , which gives the calculation accuracy  $\delta(\beta_\pi^{rc}) \approx 0.05$ .

In Fig. 5, we show the ratio of the total cross section for reaction (1) to the Born cross section. This is given as a function of gamma energy  $\omega$ , for incident pion energies 40 and 600 GeV. The histogram gives  $d\sigma^{tot}$  calculated by (9) with  $\bar{\beta}_\pi = -5$ , and the curve corresponds to  $d\sigma^{tot}$  calculated by (10), with  $\bar{\beta}_\pi = -5$  and  $\beta_\pi^{rc} = -0.20$ . It is clear that both calculations are in agreement. The value of  $\beta_\pi^{rc}$  also agrees with the results presented in [13]. The same analysis was done assuming that  $\bar{\alpha}_\pi = \bar{\beta}_\pi = 0$ , and we again find  $\beta_\pi^{rc} \approx -0.20$ . This last result is important, showing that the radiative corrections simulate  $\beta_\pi^{rc} \approx -0.20$ , independent of the  $\bar{\beta}_\pi$  value.

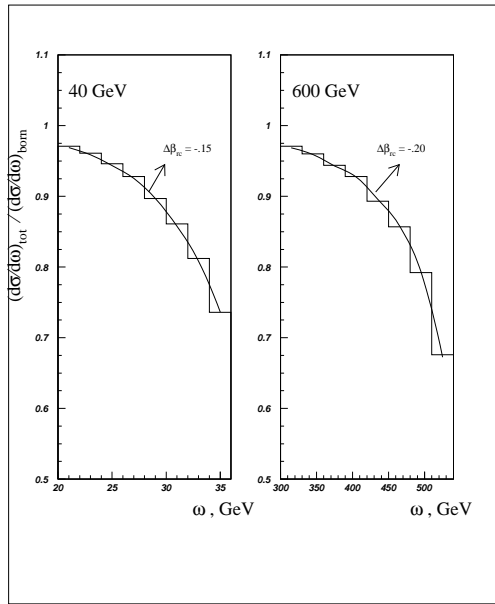


Figure 5: The ratio of the total cross section to the Born cross section as a function of detected gamma energy  $\omega$ .

One calculation with  $\bar{\beta}_\pi = -5$  was carried out to study radiative corrections to pion radiative scattering on lead. The Born and polarizability cross sections show the  $Z^2$  dependence

expected theoretically. The ratio of radiative correction to Born and to polarizability cross sections was practically unchanged compared to carbon. This is because  $\delta(\omega)$  is practically independent of  $Z$ . Only the contribution from rescattering has a  $Z$  dependence, and this is a very small contribution to the total RC.

We now summarize the main results of our RC study. The radiative corrections simulate a polarizability effect at the level of  $\beta_\pi^{rc} \sim -0.20$ . This result is for pion incident energies from 40 to 600 GeV, and for nuclei from carbon to lead. We find for  $\beta_\pi^{rc} \approx -0.20 \pm 0.05$  at 40 and 600 GeV, for  $\bar{\beta}_\pi$  from the interval  $(-7; -2)$ , the relative contribution to the polarizability from radiative corrections equals  $\beta_\pi^{rc}/\bar{\beta}_\pi \approx (3-10)\%$ . Therefore, we give a simple lowest order method of obtaining the polarizability from experimental data. We write the cross section as a sum of Born and polarizability cross sections:

$$d\sigma^{exp} = d\sigma^{Born} + \bar{\beta}_\pi^{exp} d\sigma^m. \quad (15)$$

We now find the best fit  $\bar{\beta}_\pi^{exp}$  for  $d\sigma^{exp}$  using RCFORGV, or any other convenient fit program. This experimental  $\bar{\beta}_\pi^{exp}$  must be corrected by  $\beta_\pi^{rc}$ . We have by comparison to (10), the relationship:  $\bar{\beta}_\pi^{exp} = \bar{\beta}_\pi - \beta_\pi^{rc}$ . Thus a value  $\bar{\beta}_\pi^{exp} = -5.20$  would correspond a polarizability  $\bar{\beta}_\pi = -5$ . A more exact determination would require analysis of the data with RCFORGV.

## 4 Different Born cross section calculations

In this section, we briefly describe two methods for the Born cross section calculation. The first is an exact calculation performed with the help of the RCFORGV program, and the second is the equivalent photon approximation (EPA) (Weizsäcker-Williams's method) [16, 17].

The exact calculation method consists of an accurate counting of the contributions from the all QED diagrams in the lowest order of  $\alpha$ . This corresponds to the scattering of a spinless pointlike particle by a Coulomb center with hard photon emission. The exact calculation takes into account the magnitude of the photon virtuality  $k^2$ . The exact expression of the Born cross section of the process (1) has the following form [12]:

$$\frac{d^2\sigma^{Born}}{dE_2 dQ^2} = \frac{Z^2 \alpha^3}{\vec{p}_1^2} \int_{t_{min}}^{t_{max}} \frac{dt}{t^2} S^0(t). \quad (16)$$

The explicit form of the function  $S^0(t)$  and the kinematical limits  $t_{min,max}$  are given in [11, 12]. Here we emphasize that the exact Born cross section calculation includes the contribution of the logarithmic term  $\sim \ln(t_{max}/t_{min})$  (leading logarithmic approximation), and the additional contribution of the next term which is proportional to  $\sim (1/t_{min} - 1/t_{max})$ .

The EPA method is based on the assumption that the photon virtuality is very small,  $-k^2 \leq \bar{t} \ll m_\pi^2$ . Therefore, one ignores the small deviation from the real photon, and one takes only the leading logarithmic term. In this case, the cross section of the reaction (1) can be expressed via the cross section for the  $\gamma\pi$  scattering (2):

$$d\sigma_{\pi Z \rightarrow \pi\gamma Z} = n(s_1) ds_1 d\sigma_{\gamma\pi}(s_1). \quad (17)$$

Here,  $d\sigma_{\gamma\pi}(s_1)$  is the cross section of the Compton scattering of the real photon,  $n(s_1)$  is the equivalent photon density .

In the EPA, the cross section for the reaction (1) in the center of mass frame can be written:

$$\frac{d^2\sigma^{WW}}{ds_1 d\cos\theta^*} = \frac{\alpha}{\pi} \frac{Z^2}{s_1 - m_\pi^2} \left[ \ln \frac{t_{max}}{t_{min}} + \frac{t_{min}}{t_{max}} - 1 \right] \frac{d\sigma_{\gamma\pi}}{d\cos\theta^*}(s_1), \quad (18)$$

where  $d\sigma_{\gamma\pi}(s_1)/dcos\theta^*$  is the unpolarized differential cross section of the reaction (2).

The Born cross section of the  $\gamma\pi$  Compton scattering has the form [18] :

$$\frac{d\sigma_{\gamma\pi}^{Born}}{dcos\theta^*}(s_1) = \frac{\pi\alpha^2}{s_1} \left[ 1 + \left[ -1 + \frac{2m_\pi^2 t_1}{(s_1 - m_\pi^2)(u_1 - m_\pi^2)} \right]^2 \right], \quad (19)$$

where  $t_1 = (p_1 - p_2)^2$ ,  $u_1 = (p_1 - k')^2$ .

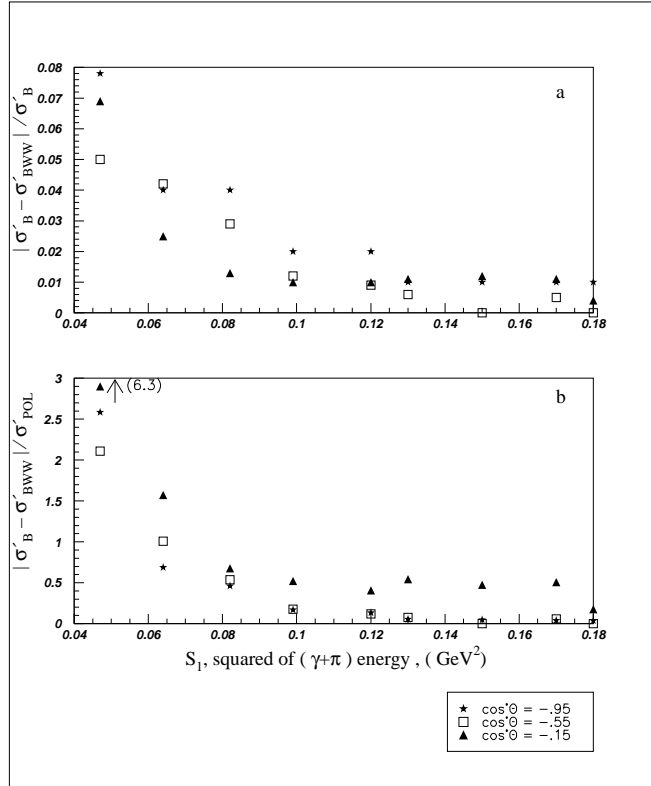


Figure 6: Comparison of two Born cross section calculations: exact calculation and EPA method ( $\sigma' \equiv d^2\sigma/dE_2dQ^2$ ).

A comparison between the two Born cross section calculations was carried out in order to estimate their applicability. In Fig. 6a the difference between the two double differential cross sections  $d^2\sigma/dE_2dQ^2$ , is presented. The superscript *Born* refers to the exact Born cross section performed by RCFORGV program, and *WW* to the Born cross section calculated by the EPA method. As in Fig. 4, ratios of  $d^2\sigma/dE_2dQ^2$  were taken, but the labeling is according to the CM variables  $s_1$  and  $cos\theta^*$ . The cross section difference is given with respect to the exact Born cross section.

From Fig. 6a, we can see that the EPA method agrees with the exact Born calculation with a precision better than 3 % in the kinematical region  $s_1 \geq 0.13 GeV^2$  and at backward scattering angles  $cos\theta^* \leq -0.5$ . From Fig. 6b, the cross sections difference divided by the polarizability cross section is displayed. In the kinematical range limited by the inequalities  $s_1 \geq 0.13 GeV^2$  and  $cos\theta^* \leq -0.5$ , both Born cross section calculation methods are in agreement and can be applied equally well. This kinematical region was also preferred for the study of the magnetic polarizability (see section 3).

The validity of the EPA method was discussed in recent papers (see for example [19]-[21]) shown that the EPA for the other processes can lead to large errors, if used outside of the region of applicability and must be used judiciously or improved in order to get correct results.

## 5 Conclusions

We used the semi-analytical program RCFORGV to evaluate the contribution of the radiative corrections to the total cross section of the pion scattering by a Coulomb center with hard photon emission. We showed that the radiative corrections can simulate the polarizability effect and the average effect  $\beta_{\pi}^{rc} = (-0.20 \pm 0.05) \times 10^{-43} \text{cm}^3$  was obtained. We showed that the preferred kinematical region to investigate the magnetic polarizability cross section in the laboratory frame is the range of final gamma energy  $\omega \geq 0.75E_1$ . The corresponding range in the center of mass frame is defined by the following inequalities :  $s_1 \geq 0.15 \text{GeV}^2$  and  $\cos\theta^* \leq -0.75$ , where  $s_1$  and  $\theta^*$  are the energy squared and the polar scattering angle. The cross sections of the reaction (1) computed in the Born approximation using the exact calculation method and the equivalent photon approximation are in the agreement for hard emitted photons  $\omega \geq 0.75E_1$ . In the range of the photons  $\omega \leq 0.6E_1$ , we must use the exact calculation method. The suggested method allows to take into account the radiative correction effects with high accuracy.

## Acknowledgements

We would like to thank D. Bardin, E. Gurvich, G. Mitsel'makher, A. Ol'shevsky and L. Frankfurt for numerous helpful discussions. A. A. thanks the Tel Aviv University group for the opportunity to visit and work in Tel Aviv on this project, and Professor Abdus Salam, the International Atomic Energy Agency and UNESCO for hospitality at the International Centre for Theoretical Physics, Trieste.

This work was supported by the Yuval Ne'eman chair of Theoretical Physics at Tel Aviv University, the Ministry of Absorption, the Israel Ministry of Science, the Wolfson Foundation and the U.S.-Israel Binational Science Foundation (B.S.F.), Jerusalem, Israel.

## References

- [1] A. Klein, *Phys. Rev.* **99** (1955) 998.
- [2] A. M. Baldin, *Nucl. Phys.* **18** (1960) 310.
- [3] V. A. Petrun'kin, *Sov. J. Part. Nucl.* **12** (1981) 278.
- [4] A. I. L'vov, *Sov. J. Nucl. Phys.* **42** (1985) 583.
- [5] B. R. Holstein, *Comments Nucl. Part. Phys.* **19** (1990) 239.
- [6] J. F. Donoghue and B. R. Holstein, *Phys. Rev.* **40D** (1989) 2378.
- [7] A. S. Galperin et al., *Sov. J. Nucl. Phys.* **32** (1980) 545.
- [8] Yu. M. Antipov et al., *JETP Letters* **35** (1982) 375;  
Yu. M. Antipov et al., *Z. Physik* **C24** (1984) 39.
- [9] Yu. M. Antipov et al., *Phys. Letters* **B121** (1983) 445;  
Yu. M. Antipov et al., *Z. Physik* **C26** (1985) 495.
- [10] M. A. Moinester, in: W. Van Oers (eds.), Proceedings of the Conference on the Intersections between Particle and Nuclear Physics, Tucson, Arizona, 1991 (AIP Conference Proceedings 243, 1992) p.553.
- [11] A. A. Akhundov and D. Yu. Bardin, JINR Dubna preprint P2-82-650 (1982).
- [12] A. A. Akhundov, D. Yu. Bardin and G. V. Mitsel'makher, *Sov. J. Nucl. Phys.* **37** (1983) 217.
- [13] A. A. Akhundov, D. Yu. Bardin, G. V. Mitsel'makher and A. G. Ol'shevsky, *Sov. J. Nucl. Phys.* **42** (1984) 426.
- [14] A. A. Akhundov and D. Yu. Bardin, Fortran program RCFORGV and JINR Dubna preprint P2-82-650 (1982).
- [15] M. Veltman, SCHOONSCHIP - *A Program for Symbol Handling*;  
H. Strubbe, *Comp. Phys. Comm.* **8** (1974) 1.
- [16] K. F. von Weizsäcker, *Z. Physik* **88** (1934) 612;  
E. J. Williams, *Phys. Rev.* **45** (1934) 729.
- [17] A. I. Akhieser, V. M. Berestetski, *Quantum electrodynamics* (Nauka, Moscow, 1981).
- [18] D. Babusci, S. Bellucci, G. Giordano, G. Matone, A. M. Sandorfi and M. A. Moinester, *Phys. Letters* **B277** (1992) 158.
- [19] V. M. Budnev et al., *Phys. Rep.* **C15** (1975) 181.
- [20] S. Frixione et al, CERN preprint CERN-TH.7032/93 (1993).
- [21] M. Drees and R. M. Godbole, Wisconsin University preprint MAD-PH-819, BU-TH-94-02 (1994).